FRAMEWORK FOR A SYSTEM-WIDE DAM RISK REDUCTION PROGRAM IN NORTHERN CALIFORNIA

Jennifer L Donahue
Geosyntec Consultants, San Francisco, CA, USA
Kathryn E. Wooddell
Sr. Seismologist Pacific Gas and Electric Company, San Francisco, CA, USA

ABSTRACT

The need for evaluating and implementing a long-term seismic risk program for a hydroelectric system includes over 170 dams in California. The program objective is to rank all dams in the portfolio in terms of risk while simultaneously quantifying the uncertainty of the risk estimates for each dam and for the full portfolio of dams such that the risk mitigation projects can be prioritized based on quantitative risk estimates. The approaches used to capture the uncertainties in the source characterization, ground-motion characterization, and dam fragility characterization are summarized. A key issue for use of seismic risk in risk-informed decision-making is the large epistemic uncertainties in the estimated risk values due to the large uncertainties in the seismic hazard inputs and the dam fragility inputs. Examples of methods for showing the sensitivity of the hazard or the risk to uncertainty in the source characterization, ground-motion characterization, dam response model, and dam fragility model are shown. Tornado plots are useful for the sensitivity for individual dams and portfolio sensitivity plots are useful for showing the number of dams that are affected by a particular parameter of the model. These methods can be used to quantify the uncertainty and relative importance of each input parameter in terms of its contribution to the risk at each dam. The parameters can then be ranked in terms of their overall impact to the risk estimates for the portfolio of dams. The ranked list can be used to prioritize future seismic research that will lead to the greatest reduction in uncertainty in seismic risk. Ultimately, the goal is to have quantitative estimates of the seismic risk with small enough uncertainties such that the risk estimates provide useful information for prioritizing risk mitigation projects as part of a long-term risk reduction program.

1 INTRODUCTION

A client maintains a portfolio of 172 dams throughout its service territory. Rather than only considering the current regulatory requirements, the client is evaluating the use of a long-term risk-reduction approach for its dam portfolio. A long-term risk reduction program would seek to systematically reduce the risk for the portfolio of dams over a time period of decades. Dams have numerous risks from earthquakes, floods, and operator error, to name a few. In the initial evaluation of a risk-reduction approach described in this paper, only the seismic risk part is being addressed. The flood and operator error risks will be considered in subsequent evaluations of the risk-reduction approach.

In a long-term risk reduction program, the goal is to optimize the use of available annual funding for risk mitigation so that the greatest risk reduction in portfolio risk is achieved in the shortest time. In addition, it is also desirable to be able to demonstrate the relation between risk reduction and mitigation cost. These two objectives require quantitative methods for computing the risk at individual dams and for the full portfolio of dams. While there are accepted methods for computing seismic risk, the resulting seismic risk estimates have very large epistemic uncertainties leading to potentially small differences between dams making it very difficult to rank risk for the entire portfolio. This makes it difficult to distinguish between the risks at different dams when prioritizing risk mitigation projects based on optimizing risk reduction.

Given the timeframe of this type of long-term risk reduction program, there is an opportunity to conduct research to improve the seismic hazard (source characterization and ground-motion models) and the dam fragility models and significantly reduce the epistemic uncertainty in the risk during the life of the program. With reduced uncertainties in the risk estimates, the prioritization of risk mitigation projects can be better optimized. In this paper, we describe a methodology for identifying research topics that lead to the largest reduction in risk uncertainty. If the risk uncertainty is not fully developed, the hazard uncertainty can be used as a rough proxy for risk uncertainty because the risk scales with the hazard.

Figure 1 shows the location of the 172 dams in the portfolio (yellow triangles), and a base-map of the faults is shown in blue. The fault database in Figure 1 draws upon over 50 years of geologic investigations. The client maintains a fault model based on published information and a sensitivity model for new and emerging information prior publication. The technical details of the parameters included in this characterization are discussed in Section 2.1. A gridded seismicity model is used to address earthquake ruptures that occur off known faults in the service territory.

2 METHODOLOGY

The characterization of risk at any one dam requires two main analyses, a probabilistic seismic hazard analysis (PSHA) and a risk analysis. Each analysis requires two sources of input that are described below.

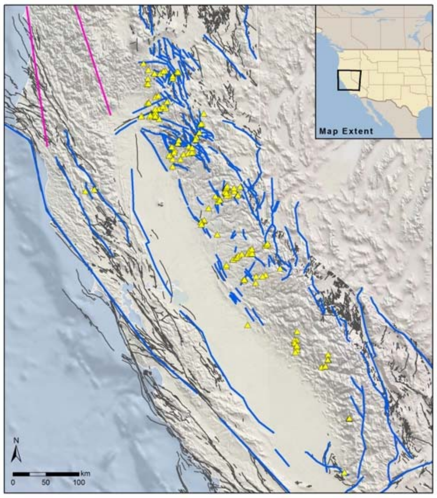

Figure 1. Location of the client's dams and faults contributing to hazard throughout Northern and Central California

Inputs for the PSHA include the seismic source characterization (SSC) and the ground-motion characterization (GMC). The output of the PSHA is a hazard curve that describes the annual rate of exceeding a suite of ground motion levels for a selected response spectral period.

Inputs for the risk analysis are the hazard curve, the dam response model (e.g. deformation), and the fragility curve for failure of the dam (probability of failure given the deformation).

2.1 Seismic Source Characterization

The Seismic Source Characterization (SSC) is described by a logic tree that provides the parameters necessary to characterize the fault source parameters for each of the models necessary to compute the PSHA. Each node of the logic tree includes alternative branches that capture the epistemic uncertainty in either models or model parameters. A weight is assigned to each branch. In each case, the alternate branches are intended to represent the scientific uncertainty in the model or parameter that arises from a limited data or knowledge (i.e. the epistemic uncertainty) (Bommer and Scherbaum, 2008), and the weights on the branches contributing to each node sum to one.

2.1.1 SSC Logic Tree for Crustal Sources

The structure of the SSC logic tree for crustal fault sources is shown in Figure 2. It includes a total of seven nodes for each fault source: the equivalent Poisson ratio, the fault dip, the maximum depth of faulting, the slip rate, the form of the magnitude probability density function (PDF), the mean characteristic magnitude, and the maximum magnitude. The role of each node in the PSHA calculation is summarized below, but an in-depth technical discussion of each parameter is intentionally withheld, as the SSC model is not the focus of this paper.

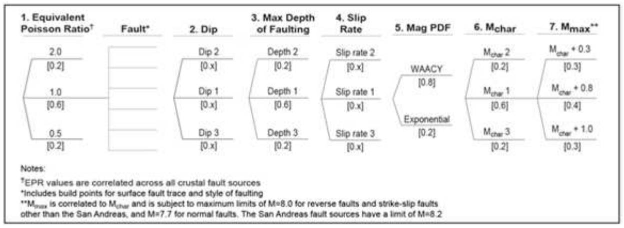

Notes:
†EPR values are correlated across all crustal fault sources
*Includes build points for surface fault trace and style of faulting
**M_{max} is correlated to M_{char} and is subject to maximum limits of M=8.0 for reverse faults and strike-slip faults other than the San Andreas, and M=7.7 for normal faults. The San Andreas fault sources have a limit of M=8.2

Figure 2. Logic Tree Structure for PSHA for All Crustal Fault Sources in the SSC Model

The equivalent Poisson ratio (node 1) addresses the time-dependence of earthquake ruptures. Commonly in PSHA, earthquake recurrence is modeled as a time-independent Poisson process, meaning that earthquakes occur randomly in time over a long interval. Thus, knowing when a previous hazard significant earthquake occurred gives no additional predictive power to the model. Multipliers greater than one mean that the fault rupture is more likely to occur than its long-term rate (the fault is overdue for rupture). Conversely, multipliers less than one mean that the fault rupture is less likely to occur than its long-term rate.

The fault dip (node 2) describes the angle from horizontal of the fault plane. The maximum depth of faulting (node 3) defines the vertical depth over which fault ruptures are allowed to occur in the model. Taken together, nodes 2 and 3 define the geometry of the fault. Nodes 4, 5, 6, and 7 set the parameters used for computing the rates of a given magnitude. The slip rate (node 4) represents the net slip on the fault plane. The magnitude PDF (node 5) provides the functional form of the magnitude-frequency distribution for earthquake magnitudes originating on a single source; and it is anchored over the appropriate magnitude range through the mean characteristic magnitude (M_{char}) (node 6). The maximum magnitude (M_{max}) (node 7) is used to define where the magnitude PDF is truncated, and it represents the largest magnitude that can occur on a fault source given M_{char}.

2.1.2 SSC Logic Tree for Cascadia Interface Source

The SSC logic tree for the Cascadia interface source is shown in Figure 3. It includes four nodes: the location of the eastern edge of the interface, the recurrence interval, the magnitude PDF, and the magnitude of the characteristic rupture.

Two alternative locations for the eastern (down-dip) edge of the Cascadia interface are considered (node 1) based on the 2014 USGS National Seismic Hazard Map (NSHM) model (Petersen et al., 2014). This down dip edge controls the closest distance from the client's dams to the Cascadia interface.

The rates of the expected ground motions are defined through nodes 2, 3, and 4. The recurrence interval (node 2) describes the mean time between characteristic earthquakes. The magnitude PDF (node 3) provides the functional form of the magnitude-frequency distribution, and it is anchored over the appropriate magnitude range through the mean characteristic magnitude (node 4).

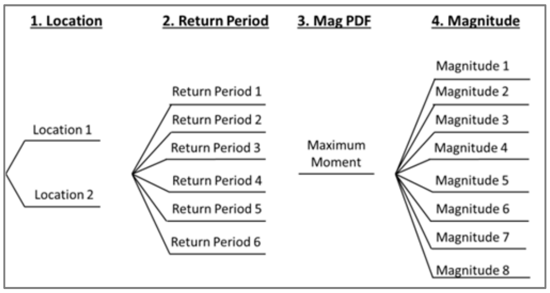

Figure 3. Logic Tree Structure for PSHA for Cascadia Subduction Zone Interface Source in the SSC Model

2.2 Ground Motion Characterization

The Ground Motion Characterization (GMC) is a logic tree that provides the ground-motion models used to compute the ground motion for a given earthquake scenario. The structure of the GMC logic trees, shown in Figure 4, is the same for the two crustal source regions and the subduction sources. The first node captures the alternative GMPEs for the base scaling of the median ground motion (e.g. magnitude, distance, V_{S30} scaling). The branches sample the alternative GMPEs that are considered applicable for the median. For the transpressional regime (Figure 5), the five NGA-West2 models are used. For the extensional regime, the branches for the GMPEs used the models from the Southwestern U.S. (SWUS) ground motion project for the Palo Verde site in Arizona (GeoPentech, 2015). For the subduction source, the GMPEs are selected from the BCHydro model (Abrahamson et al, 2016) using the three alternative large magnitude scaling options as the three base GMPEs for the median.

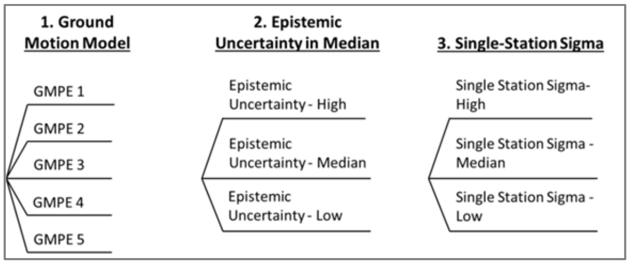

Figure 4. Logic Tree Structure for PSHA for Crustal and Subduction Fault Sources in the GMC Model

The second node captures the additional epistemic uncertainty in the median due to the limited data available and represents the statistical uncertainty in the empirical GMPEs (e.g. Al Atik and Youngs, 2013) as well as the potential for regional differences in the median ground motion (e.g. non-ergodic effects). For the subduction models, the additional epistemic uncertainty was adopted from Abrahamson et al (2016) which represents the differences in the medians observed for different subduction regions around the world (e.g. non-ergodic effects)

The third node captures the aleatory standard deviation of the ground motion. The single-station sigma approach (GeoPentech, 2015) is used to allow for use of site-specific site response analysis to be used without double counting the site effects. The SWUS models and weights for single station sigma are used for the crustal earthquakes. The BCHydro models and weights are used for the alternative single-station sigma for subduction earthquakes.

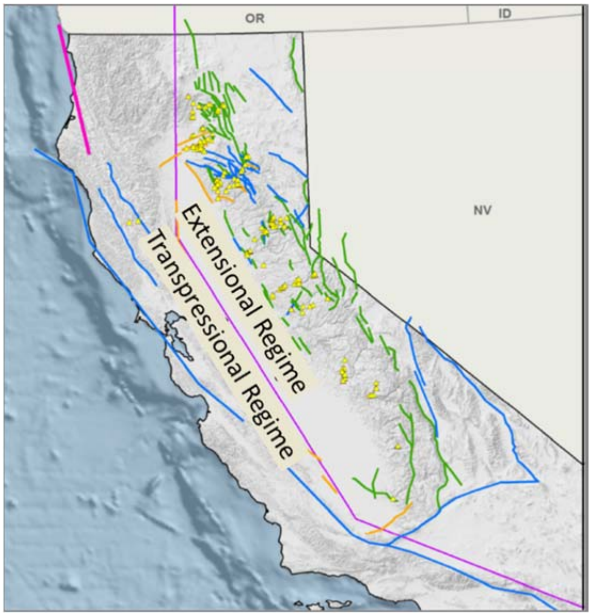

Figure 5. Transpressional and Extensional Regimes for the GMC Crustal Fault Sources. Strike-slip faults shown as blue lines, reverse faults as orange lines, normal faults as green lines, and Cascadia as magenta

2.3 Hazard Analysis

The SSC and the GMC characterization logic trees provide the input for the PSHA. The hazard is computed using the PSHA software Haz45 (www.github.com/abrahamson/Haz), to compute the hazard at each of the 172 dam sites. Haz45 computes the hazard by stepping through the logic tree and computing the rate of exceeding the specified ground motion amplitudes for each of the specified spectral accelerations for every possible combination of logic tree branches for each source. The rates of exceedance from the difference sources are then summed, and the result is a suite of hazard curves describing the annual rate of exceeding a specified ground motion level for the each of the spectral periods of interest.

A post-processor was developed to rapidly summarize the hazard output for each facility and provide an easy way to compare the output between dams. Figure 6 shows an example of the output obtained from this post-processor that includes an index map with the site location, a suite of mean hazard curves, including both the total hazard curve and marginal contributions from the most hazard significant faults, a deaggregation of the hazard showing the hazard contribution as a function of magnitude and distance, and a tornado plot summarizing the top sources of uncertainty in the hazard analysis. Further explanation of the tornado plot is provided in Section 2.3.1. At each dam site, a total of four plots of this type are produced showing the results for each of the two spectral periods at two selected hazard levels of interest. For the purposes of this project, we have chosen 10^{-3} and 10^{-4}.

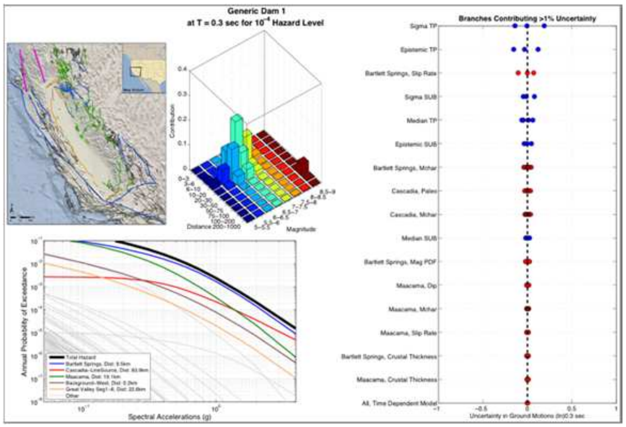

Figure 6. Summary plot of hazard results. Includes index map with the site location, a suite of mean hazard curves, deaggregation of the hazard, and a tornado plot

2.3.1 Explanation of tornado plot

A tornado plot is a visual tool that makes it easy to determine, with only a quick glance, which parameters contribute the largest uncertainty to the hazard. They are created from the full suite of hazard sensitivity results for a given period and at a given hazard level.

Figure 7 shows how a tornado plot is developed from a suite of hazard curves. The bold black line is the base-case model. The base-case is the total mean hazard curve derived after computing all combinations of the SSC and GMC logic trees with their weights. The other hazard curves in Figure 7 are alternative mean hazard curves resulting from selecting a particular branch for a particular node of the logic tree. For example, a sensitivity on the time dependent model is conducted by first replacing one branch in the time dependent model node with a weight of 1 and assigning all other branches in this node a weight of 0. Because the time dependent model node contains 3 branches, this results the three alternative hazard curves.

Once the full suite of hazard curves is computed, a hazard level that is appropriate for the project is selected. In this example, a hazard level of 10^{-4} is used. The ratio of ground motion at the target hazard level for each branch to the base-case is computed, resulting in three points that summarize the amount of uncertainty in a particular parameter, for this example, the time-dependent model.

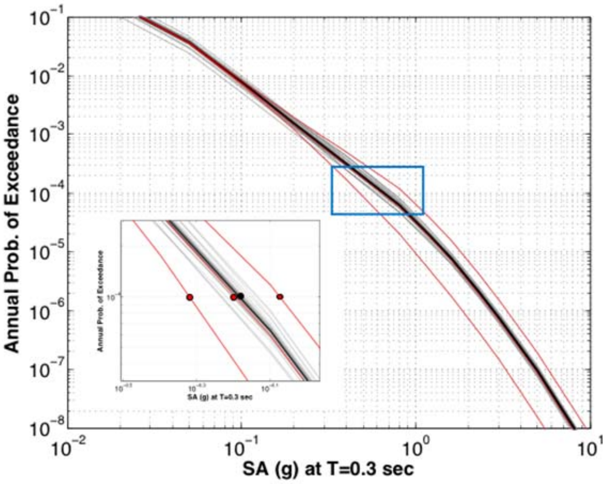

Figure 7. Example Hazard Curves with base-case model (black line) is compared with a specific sensitivity case (red line). Black and red dots mark the spectral acceleration at a hazard level of 10^{-4}

When sorted such that the parameters with the greatest uncertainties are at the top and the parameters with the least uncertainty are at the bottom, the figure resembles a tornado in shape (Figure 8). Tornado plots can either be computed to show uncertainty in ground motion at a given hazard level, as we have done in this case, or uncertainty in hazard at a given ground-motion value. We have chosen to show the uncertainty in natural log of the ground motion. The relationship between the uncertainty in the ground motion and hazard depends on the slope of the hazard curves. For this case, with a slope near 3, the hazard uncertainty (in natural log units) is approximately three times the ground-motion uncertainty (if the ground-motion uncertainty is 0.3 LN units, then the hazard uncertainty is about 0.9 LN units).

If we used the results shown in Figure 8 to identify SSC research that would lead to the largest reduction in the uncertainty in the hazard at this dam (based on improved SSC model parameters only), we would select the time-dependence (equivalent Poisson rate), the background zone rate, and the slip rate of the nearby Maidu fault as the topics for research. The tornado plot in Figure 8 considers only the hazard at one dam. When considering the full portfolio of dams, the impacts on the hazard (and risk) at multiple dams should be considered in evaluating which SSC research is the highest priority. That is, SSC parameters that affect more than one dam are likely to be higher priority than SSC parameters that affect only one dam.

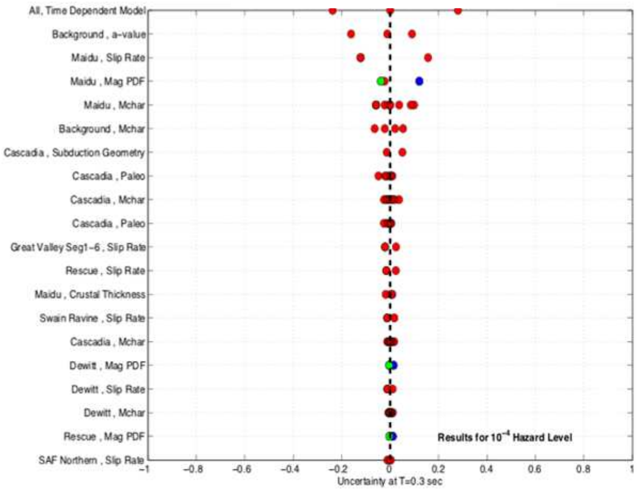

Figure 8. Example Tornado Plot of all SSC parameters for a generic site at a hazard level of 10^{-4}. The x-axis shows the natural log units of the ground motion ratio.

2.3.2 Use of Cloud Computing for PSHA

Given the large number of fault sources and the numerous alternative branches in the logic trees, we found that it took between 4.5 to 6 hours to compute the hazard for a single dam. Assuming the hazard analyst has a quad-core computer; three sites can reasonably be run at a time, meaning it would take approximately 344 hours (over 14 days) of straight computation time to complete the hazard analyses. For these reasons, non-traditional means of processing data were required and the hazard analysts utilized “the Cloud” for the rigorous PSHA computations.

Cloud computing is a recently emerged model which is becoming popular among almost all enterprises. Using the Cloud architecture addresses three key difficulties surrounding large-scale data processing; it eliminates the need for multiple machines, it is available on demand, and it is scalable.

Utilizing Amazon Web Services (AWS), the hazard analysts developed and used two Elastic Cloud Compute (EC2) Instances to run all analyses. One instance is the equivalent of a 40-core computer and this allows for a maximum of 38 runs per instance. Using AWS with two of the large 40-core processors, all 172 sites with two periods each, could be efficiently run in less than 14 hours.

The cost of running an EC2 instance is currently \$4.04/hour. There is also a small charge for storing data on the cloud of \$0.12/Gigabyte/month.

2.4 Dam Fragility Characterization

Fragility curves for dams describe the Probability of Uncontrolled Rapid Release of Water (URRW) given a percentage in crest deformation (Figure 9). For this project, the fragility curves were developed for generic dam types by Dr. Jennie Watson-Lamprey.

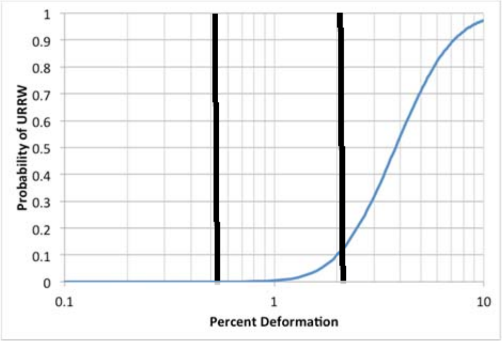

Figure 9. Example Fragility Curve for an embankment dam showing probability of URRW versus percent deformation of dam height. Solid black lines correspond to 0% probability of URRW at 0.5% and 10% probability at 2% deformation.

The parameterization of the fragility curves is shown in the Dam Fragility Curve (DFC) logic tree (Figure 10). The five nodes of the logic tree are designed to capture the uncertainty in the DFC parameters: the dam fundamental period (node 1), dam yield acceleration (node 2), the dam response model (node 3), the fragility curve anchor point (node 4), and the slope of the fragility curves given in terms of the sigma of a cumulative lognormal distribution (node 5).

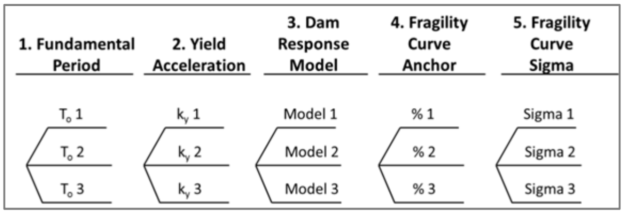

Figure 10. Logic Tree Structure for Dam Fragility Characterization for Risk Modeling

Simplified dam response models and fragility models are currently under development. Additional features and parameters will be incorporated into the current simplified model as necessary. To demonstrate the process, the following central values are assumed for the initial risk calculations: a deformation of 2% of the dam heights corresponds to 10% probability of URRW (node 4); the shape of the fragility curve is a cumulative lognormal distribution with a standard deviation of 0.5 LN units (node 5); and the probability of URRW is 0 for deformation less than 0.5% of the dam height. These assumed values are for this example only, and should not be used for risk-informed decision-making. A broad uncertainty range was applied to each of these assumed central values as well as the fundamental period and the yield acceleration for use in the sensitivity studies only.

2.5 Initial Risk Analysis

The DFC characterization logic tree provides one of the inputs for the risk analysis. The probability of failure is computed by integrating the conditional probability of failure (given the deformation) over all possible ground-motion levels and all possible deformations for the ground-motion level and selected dam properties. An example of the seismic risk and the epistemic uncertainty for two dams is shown in Figure 11. The mean risk for each dam is shown by the red point and the epistemic uncertainty (5-95% range) is shown by the blue error bars. Although dam 1 has a mean risk that is twice as large as dam 2, the uncertainties are so large that the difference is not robust. This indicates the need for reduction of the uncertainty in the risk estimates to allow for more unique solutions, with less overlap. This will ease the ranking of the risk and prioritization of future mitigation projects.

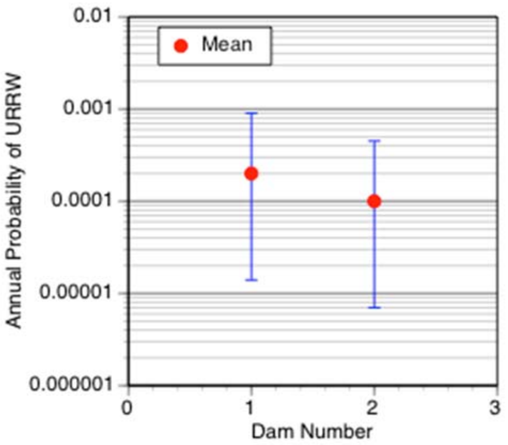

Figure 11. Example of Risk estimates using annual probability for failure versus consequences for two example dams.

The tornado plot approach was also used to determine which parameters lead to the large uncertainty in risk. Figure 12 shows the sensitivities to DFC parameters compared to the sensitivities to GMC and SSC parameters, plotted as a tornado plot in Figure 12. For the dam in this example, the uncertainty in the yield acceleration leads to the largest uncertainties in the risk; however, the assumed uncertainty range for the yield acceleration is assumed and not well constrained.

With the many tornado plots for SSC, GMC, and Risk, an additional tool was needed to distill the results. As part of the prioritization of research to reduce uncertainty in risk, the client needs to consider the impact on the risk estimates for the full portfolio of dams. There may be cases in which a specific parameter leads to large uncertainty for one dam whereas another parameter leads to moderate uncertainty at multiple dams. Would it be better to spend research funds to reduce uncertainty in risk for a few dams; or spend funds on a parameter that affects the many dams?

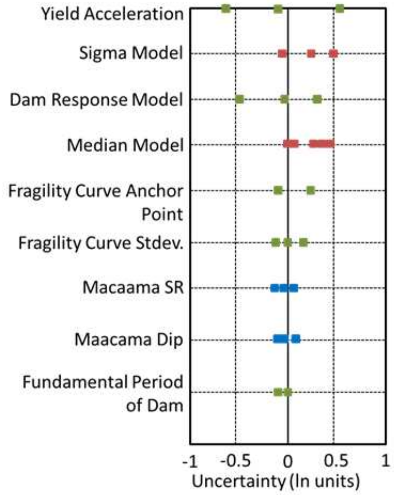

Figure 12. Example Tornado Plot of the sensitivity of the seismic risk. SSC parameters (blue squares), GMC parameters (red squares), and DFC parameters (green squares) that have the greatest impact on the epistemic uncertainty for this dam.

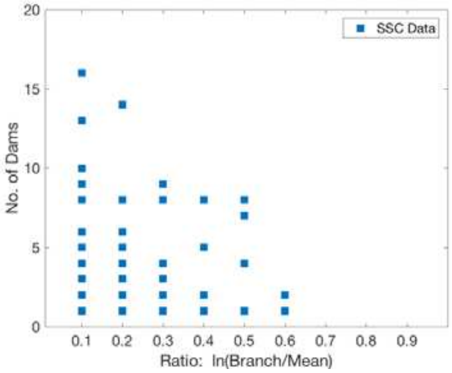

Figure 13. Example Sensitivity Plot of all SSC parameters by dam

To help identify the number of dams for which the risk is affected by a single parameter, the number of dams for which the risk changes by more than a specified value (in LN units) can be evaluated. An example of applying this approach for the ground-motion sensitivity to the SSC parameters is shown in Figure 13. The dams with changes in the 10^{-4} ground motion greater than 0.1 LN units was compiled. Each parameter for the SSC model is modeled as a blue square. The x-axis shows the ratio of the sensitivity to the mean branch of the logic tree (in LN units). The y-axis shows the number of dams that exceed the ratio from a single common SSC parameter. On the right side of the plot, a few SSC parameters lead to a large ratio of the uncertainty (0.6 LN units) but only affect one or two dams. Conversely, one of the SSC parameters affects 16 dams, yet the ratio is much smaller (0.1 LN units). Using this type of graph, coupled with similar graphs for GMC and DFC sensitivity, will help the client to prioritize the allocation of research funding for uncertainty reduction for the portfolio risk.

3 CONCLUSIONS

Dam risk provides an attractive metric for both prioritizing mitigation projects and demonstrating progress in risk reduction; however, using the current models and methods, the uncertainties in the risk estimates are very large, limiting the ability to resolve differences between the risk at different dams.

There is a need to develop improved data, models, and methods to reduce the uncertainty in the risk estimates and provide improved resolution in risk differences between dams. The tornado plots of hazard uncertainty and risk uncertainty are useful tools for identifying which research topics have the chance of leading to the largest reduction of uncertainty in risk. While it will take 5-10 years to develop significant improvements in the models and parameters that lead to significant reduction in the uncertainty of risk estimates, a long-term risk reduction program can take advantage of the improvements over the decades-long duration of the program.

4 ACKNOWLEDGEMENTS

The authors would like to acknowledge Dr. Norman Abrahamson, Dr. Jennie Watson-Lamprey, Pacific Gas and Electric Company Geosciences and Hydro Departments for their contributions and comments on the paper.

5 REFERENCES

Abrahamson, N., Gregor, N., and Addo, K. 2016. BC Hydro Ground Motion Prediction Equations for Subduction Earthquakes, *Earthquake Spectra* 32: 23-44.

Al Atik, L., and Youngs, R.R. 2013. Epistemic Uncertainty for NGA-West2 Models, PEER Report No. 2013/11, Pacific Earthquake Engineering Research Center, University of California, Berkeley, 59 pp.

Bommer, J.J., and Scherbaum, F. 2008. The Use and Misuse of Logic Trees in Probabilistic Seismic Hazard Analysis, *Earthquake Spectra* 24 (4): 997-1009.

GeoPentech 2015. Southwestern United States Ground Motion Characterization SSHAC Level 3 – Technical Report Rev 2, March.

Petersen, M. D., Moschetti, M.P., Powers, P.M., Mueller, C. S., Haller, K. M., Frankel, A. D., Zeng, Y., et al., 2014, Documentation for the 2014 Update of the United States National Seismic Hazard Maps, U.S. Geological Survey Open-File Report 2014–1091, 255 pp.